Prediction of diurnal change in 10-h fuel stick moisture content

Ralph M. Nelson, Jr.

Abstract: Several methods are available for estimating the moisture content of 10-h response time fuels in the U.S. National Fire Danger Rating System (NFDRS). These fuels are represented by an array of four 1.27 cm diameter ponderosa pine (*Pinus ponderosa* Dougl. ex Laws.) dowels weighing about 100 g when oven dry. The prediction model currently used in the NFDRS is driven by information from afternoon weather readings. To improve responsiveness of the predictions to weather change, a 10-h stick moisture content prediction model is developed that uses observations (air temperature and relative humidity, insolation, and rainfall amount) available from a remote automatic weather station (RAWS). Equations describing the transfer of heat and moisture at the surface and within a 10-h stick are derived and then solved numerically. Collection of field experimental data on weather, stick weight, and stick temperature to guide development of the model is briefly described, and predicted and observed mean moisture contents are compared. Additional 10-h stick moisture content data, collected independently, are used to test model predictions. Calculated values are sometimes outside the bounds of variability in moisture content determined from the data, suggesting the need for further tests. The model simulates diurnal change in moisture content and temperature of 10-h sticks but can be adapted to cylindrical wood sticks of any practical size.

Résumé : Dans le système national d'évaluation des dangers d'incendies des États-Unis (NFDRS), il existe plusieurs méthodes pour évaluer la teneur en humidité des combustibles à délai de réaction de 10 heures. Ces combustibles sont représentés par un assemblage de quatre bâtonnets de pin ponderosa (*Pinus ponderosa* Dougl. ex Laws.) de 1,27 cm de diamètre, dont le poids anhydre est d'environ 100 g. Le modèle de prédiction utilisé couramment dans le NFDRS est alimenté par des informations provenant de la lecture des paramètres météorologiques de l'après-midi. De manière à améliorer la sensibilité des prédictions aux variations météorologiques, on a développé un modèle de prédiction de la teneur en humidité des bâtonnets à délai de réaction de 10 heures qui utilise les observations fournies à distance par une station météorologique automatique (RAWS). Des équations décrivant le transfert de chaleur et d'humidité à la surface et à l'intérieur des bâtonnets ont été dérivées et résolues numériquement. On décrit brièvement la prise des données expérimentales de terrain sur la météo, la masse et la température des bâtonnets qui ont servi à développer le modèle. Les teneurs moyennes en humidité prédites et observées ont par la suite été comparées. Des données additionnelles sur la teneur en humidité des bâtonnets ont été prélevées indépendamment puis ont été utilisées pour tester les prédictions du modèle. Les valeurs calculées se situent parfois à l'extérieur des limites de la variabilité de la teneur en humidité obtenue dans les données, ce qui suggère la nécessité de réaliser des tests additionnels. Le modèle simule les variations journalières de la teneur en humidité et de la température des bâtonnets à délai de réaction de 10 heures mais il pourrait être ajusté à d'autres bâtonnets cylindriques en bois, peu importe la dimension.

[Traduit par la Rédaction]

Introduction

Relationships between weather and wildland dead fuel moisture content have been studied for nearly a century, but reliable methods for predicting the diurnal variation in moisture content are not yet developed. In the early days of fire research, efforts were made to simplify fuel moisture content estimation with routine weighings of surrogate fuels exposed in forest openings. In the western United States, Gisborne (1933) used an array of 1.27 cm diameter ponderosa pine (*Pinus ponderosa* Dougl. ex Laws.) dowels to indicate the moisture content of intermediate-size fuel; in the East, a surrogate consisting of three basswood (*Tilia americana* L.) slats, each 0.32 cm thick, represented light litter fuels (Jemison et al. 1949). Research on methods of estimating fuel moisture with indicator sticks continued into the 1960s (Cramer 1961; Storey 1965). During the period from about 1960 to 1980 a national system of fire danger rating evolved, culminating in the National Fire Danger Rating System (NFDRS) in use today (Deeming et al. 1977; Bradshaw et al. 1983; Burgan 1988).

The NFDRS is an assembly of indices that allows fire management personnel to quantify fire danger and assess fire potential. Dead fuels are categorized by 1-, 10-, 100-, and 1000-h moisture response classes (Bradshaw et al. 1983). The four fuel classes are represented by ponderosa pine dowels ranging from less than 0.64 to 25.4 cm in diameter (Deeming 1983). The 10-h response time fuels are dowels 1.27 cm in diameter. These fuels theoretically gain or lose moisture exponentially under standard conditions (ambient air at 80°F (27°C) and 20% relative humidity) at a rate such

Received November 16, 1999. Accepted March 15, 2000.

R.M. Nelson, Jr. U.S. Department of Agriculture, Forest Service, Rocky Mountain Research Station, Fire Sciences Laboratory, Stationed at: National Forests in North Carolina, 160-A Zillicoa Street, Asheville, NC 28801, U.S.A.
e-mail: rnelson01@fs.fed.us

Fig. 1. Standard array of 10-h fuel sticks exposed in the open above a cover of pine needle litter.

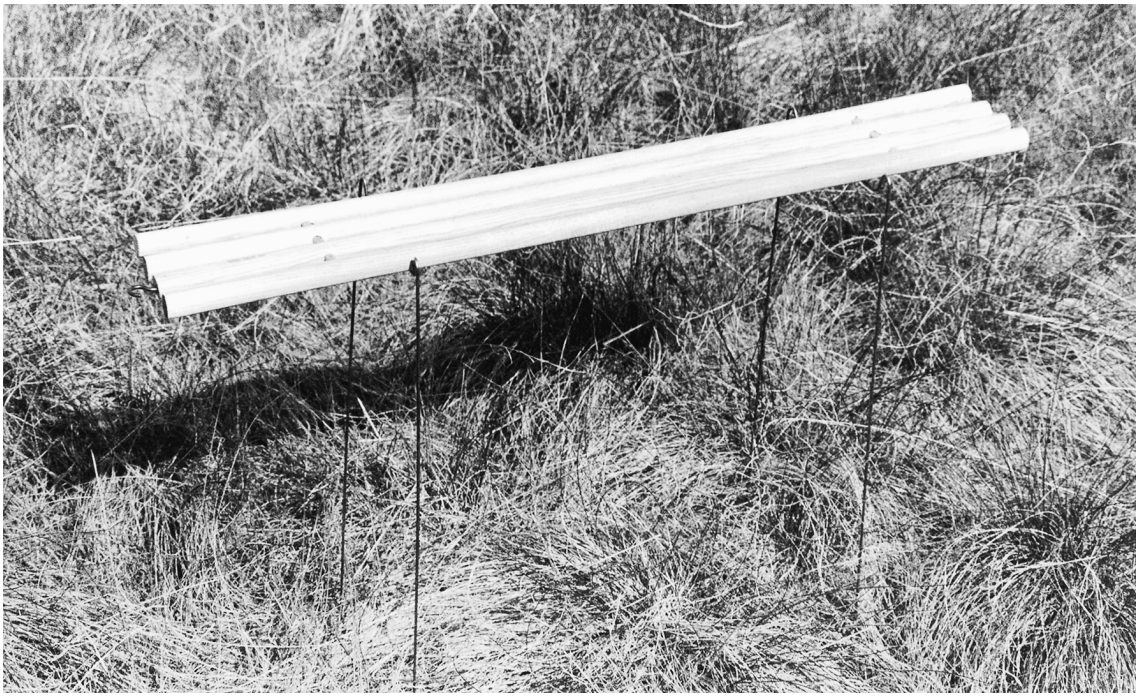

that after 10 h the exchanged moisture corresponds to $1 - e^{-1}$ (63%) of the difference between the initial and equilibrium moisture contents (Fosberg 1977). In the NFDRS, the 10-h response time is regarded as a constant property of the fuel stick; in contrast, Canadian researchers use a weather-dependent response time to describe the moisture content of litter layers (Van Wagner 1979).

The moisture content of 10-h fuel sticks currently is estimated using various approaches such as weighing, artificial sensing, and mathematical modeling. Weighing methods range from manual weighing at many fire weather stations to strain gauge systems used by the state of California. Automated weather stations now can be equipped with a fuel moisture and fuel temperature probe, which provides an estimate of 10-h stick moisture content. These estimates, with current technology, do not extend to values greater than about 30%. In a different method, an electronic fuel moisture and temperature sensor is embedded in a shortened 10-h stick and interfaced with a weather data collection platform (Parkhurst et al. 1994). The reliability of this approach at moisture contents exceeding 30% has not been demonstrated. In the modeling arena, Fosberg and Deeming (1971) and Fosberg (1977) expressed the equations of response time theory in difference form to estimate 1- and 10-h fuel moisture content. These NFDRS models are limited, however, in that their boundary conditions are computed using averaged weather data from a climatological study in O'Neill, Neb. (Fosberg and Deeming 1971). Such general methods are not well suited to describing diurnal moisture change in fine- and intermediate-size fuels. A numerical prediction model was reported by Carlson and Gay (1980) who solved equations expressing the conservation of energy and bound water in a standard 10-h stick exposed to solar and terrestrial radiation. Their model does not include rainfall or condensation and evaporation of free water. Clearly, there is no universally accepted method for evaluating 10-h moisture content over its range of practical interest from near oven dry to about 60%. A physically based numerical model would provide this capability, eliminate weighing of sticks and problems with mass loss due to weathering (Haines and Frost 1978), utilize RAWS observations to improve NFDRS 10-h fuel moisture predictions, and provide predictions in near real time.

This paper describes a model for predicting diurnal moisture content change in 10-h fuel sticks from periodically observed weather variables. The equations governing internal moisture transport are written, boundary conditions are discussed and expressed mathematically, and then computational procedures are summarized. Two field experiments yielding data with which to tune the model are described; comparisons of measured and predicted moisture contents are presented. Next, a third field experiment is reported that involves data collected independently for assessing the predictive capabilities of the model. A comparison of observed and predicted moisture contents is given. The final section discusses possible extension of the model to predict the moisture content of 1-, 100-, and 1000-h response time fuels for use in evaluating fire danger and fire behavior.

The model

Problem overview

Consider a standard array of 10-h sticks in an open exposure, in line with true north, and 0.25 m above the ground (Finklin and Fischer 1990). Such an array consists of four parallel ponderosa pine dowels approximately 50 cm long, 1.27 cm in diameter, and separated by 0.6 cm (Fig. 1). The individual sticks are held together by wooden pins inserted through all four dowels near each end of the array and perpendicular to its length. Ovendry weight of the array is close to 100 g. The model to be developed calculates temperature

and moisture content change in a single dowel. It is assumed that location of the individual stick in the array does not affect its temperature or moisture content at any time. This is an idealization, of course, as a given stick can be partially shielded from sun, wind, or blowing rain by any adjacent stick. Because the dowel's length is many times greater than its diameter, longitudinal flows of heat and moisture are neglected. The transverse flow is modeled as parallel to the short segments of growth ring visible on the end grain of the stick (flow is through radial faces of the wood fibers). Clearly, this approach is faulty when the flow of heat or moisture is not parallel to the growth rings (flow is through tangential faces of the fibers or at an angle to the growth ring segments due to dowel geometry). The variations in flow caused by directional differences in wood structure are ignored in this one-dimensional analysis. These variations are not as large as might be expected because moisture diffusion through radial and tangential fiber faces differs by a factor of only 1.5 (Stamm 1964). At its surface, the stick undergoes radiative and convective heat transfer, moisture exchange with the environment due to condensation or evaporation of free water, water vapor diffusion, and adsorption or desorption of bound water. Internal transfers of heat and moisture are considered to be coupled only through stick temperature, but the effects of latent heat associated with gain or loss of free water at the surface are included in the energy equation boundary condition. When free water is held in cell cavities within the stick, most of the liquid flow occurs because of capillary pressure gradients induced by differences in surface tension. Some free water must move by diffusion, however, because permeability of the stick to liquid flow drops to zero (according to the capillary flow model) even though a small amount of liquid remains in the cavities. Water held within cell walls moves by bound water diffusion; vapor diffusion in the cavities contributes significantly to the flow when the moisture content fraction falls below about 0.1 (Choong 1965). Moisture transfer by capillarity and diffusion is assumed to be much slower than liquid – bound water – water vapor phase interchange, so rates of phase change need not appear in the equations describing liquid, vapor, or bound water transfer. The model is based on additional assumptions and approximations discussed in the next three sections.

Internal transport

The equation describing radial heat conduction in a long cylindrical ponderosa pine stick containing no sources or sinks is

$$[1] \qquad r\rho c\frac{\partial T}{\partial t} = \frac{\partial[rk(\partial T/\partial r)]}{\partial r}$$

where ρ is the stick mass density (400 $kg \cdot m^{-3}$), c is the stick constant-pressure specific heat (1172 $J \cdot kg^{-1} \cdot K^{-1}$), T is the stick temperature (°C), t is time (h), r is the radial distance from the stick center (r = 0; m), k is the stick thermal conductivity (377 $J \cdot m^{-1} \cdot h^{-1} \cdot K^{-1}$). In general, ρ, c, and k are dependent on moisture content, but these details are neglected on the basis that the resulting T values would differ little from those of a more complex analysis. (The ratio $k/\rho c$ tends to remain constant because all three properties increase with increasing moisture content.) The value of ρ comes from the *Wood Handbook* (Forest Products Laboratory 1987); c is from the Volbehr equation evaluated at 300K (Beall 1968); and k is from Stamm (1964).

Fig. 2. Longitudinal cross section of a softwood with cell cavities of diameter w illustrating liquid water flow in the tangential direction due to decreasing capillary potential (decreasing radii of the menisci). Cross-hatched areas are wood cell walls; perforations represent bordered pits (courtesy of the Department of Wood Science and Forest Products, Virginia Polytechnic Institute and State University, Blacksburg (Siau 1995)).

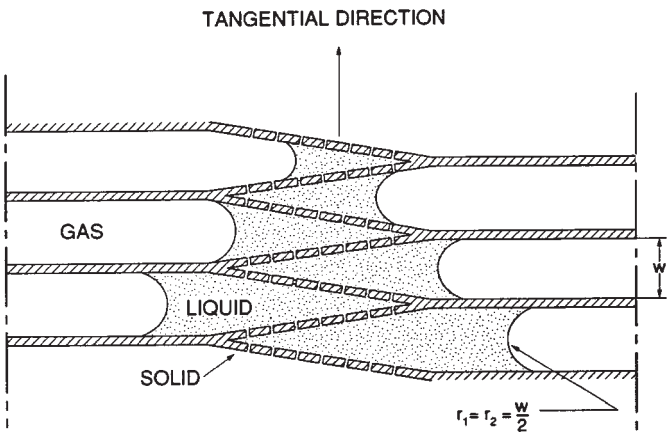

Equations describing capillary aspects of moisture transfer have not been utilized in previous studies of forest and wildland fuel moisture. Spolek and Plumb (1980) used a liquid permeability model from Comstock (1970) and certain aspects of mass transport theory to develop a model of capillary flow in softwoods. Because such flow involves only water above the fiber saturation point, they defined liquid saturation (S) as

$$[2] \qquad S = \frac{m - m_{fsp}}{m_{max} - m_{fsp}}$$

where m is the local moisture content fraction on an ovendry basis, m_{fsp} is the moisture content fraction at fiber saturation (0.3), and m_{max} is the maximum fractional moisture content the stick can attain (1.85). The value 0.3 commonly is assigned to m_{fsp}; m_{max} is computed from the stick density (Stamm 1964). Equation 2 shows that S varies from 0 to 1.

Readers interested in details of the capillary flow model are referred to Comstock (1970), Spolek and Plumb (1980, 1981), and Plumb et al. (1985); only a brief summary is presented here.

The wood cell that holds liquid water is a long tube with a roughly square cross section and tapered ends. Flow between unsaturated cells is induced by capillary pressure differences, which depend on size of the cell cavities; it takes place through small orifices (bordered pits) located only on the overlapping tapered ends of the cells. Within any two end-to-end cells with overlapping ends, menisci (one in the end of each cell) approach each other as saturation S in both cells decreases because of capillary flow. Figure 2 shows a cross section of the cell cavities of inner radii of curvature $r_1 = r_2 = w/2$ with decreasing amounts of liquid water (hence decreasing radii of the menisci) in the tangential direction.

Thus, water movement is in this direction because of the decreasing capillary potential (Siau 1995). Permeability of the stick to liquid flow, K, is determined by the critical saturation, S_c. This parameter is the value of S at which the liquid meniscus enters a tapered end of the cell cavity and is computed from details of the internal wood structure (Spolek and Plumb 1980). When $S > S_c$, the cavity region of constant size is partially filled with water, but the tapered ends are completely filled. Thus, K must take the value for saturated conditions, K_s, because the transport of water, were it to occur, would be through bordered pits on the tapered ends of the cells. In the model, this transport never takes place between cells in which $S > S_c$ because there is no difference in capillary pressure from one cell to another. Capillary flow can occur only when $S < S_c$ in one of the cells; only through flow to a region where $S < S_c$ can a cell with $S > S_c$ lose water. The way in which this flow develops is discussed below.

As S in a cell cavity decreases, eventually $S < S_c$ and the meniscus enters the end of the cavity, the radius of curvature decreases, and the capillary pressure increases (Fig. 2). The permeability becomes a function of S. Paths available for liquid flow begin to decrease until, finally, continuity of the liquid is broken and the permeability drops to zero. This occurs when $S = S_c/4$ because geometry of the wood cell dictates that menisci in the adjacent ends of the two cells no longer approach each other, but now overlap. Thus, liquid permeability of the stick is characterized as

$$[3]\qquad \frac{K}{K_s} = \begin{cases} 1, & S_c < S < 1 \\ 2\left(\dfrac{S}{S_c}\right)^{0.5} - 1, & \dfrac{S_c}{4} < S < S_c \\ 0, & 0 < S < \dfrac{S_c}{4} \end{cases}$$

where the saturation permeability K_s, determined from trials, is 2×10^{-17} m^2. The three corresponding equations describing S inside the stick, derived in Appendix A, are given by

$$[4]\qquad \begin{cases} \dfrac{\partial S}{\partial t} = 0, & S_c < S < 1 \\ r\rho(m_{max} - m_{fsp})\left(\dfrac{\partial S}{\partial t}\right) = \dfrac{\partial[(rKs/\nu w S_c)(S_c/S)^{1.5}(\partial S/\partial r)]}{\partial r}, & S_c/4 < S < S_c \\ \dfrac{\partial S}{\partial t} = 0, & 0 < S < S_c/4 \end{cases}$$

where s is the surface tension of water (9.44×10^5 kg·h^{-2}) and w the width of interior cell cavities (1.84×10^{-5} m). Values of s at 20°C and of w are taken from Shortley and Williams (1955) and Spolek and Plumb (1980), respectively. Kinematic viscosity, ν (m^2·h^{-1}), of the liquid water is given by

$$[5]\qquad \nu = 0.001\,58 + 6.37 \times 10^{-7}\,[338.76 - (T + 273.2)]^{2.1237}$$

Critical saturation S_c is 0.286 (Spolek and Plumb 1980), equivalent to a moisture content fraction of 0.743 when m_{max} is 1.85 and m_{fsp} is 0.3 (Stamm 1964).

Equations 4 indicate that capillary flow occurs locally in a limited range of S, from 0.0715 to 0.286. Flow at greater S values (the first of eqs. 4) is zero, because water is present in the square region of a given cavity, and all such cavities are the same size. In this case, a gradient in S must be established at the surface and work its way toward the stick center if water is to flow by capillarity. Furthermore, the surface value of S must be smaller than S_c. If the surface value of S falls below $S_c/4$, flow by diffusion is established in the outer regions of the stick, but capillary flow is still occurring within the inner regions. At such times, water loss from the stick is controlled by diffusion. For small S values (the third of eqs. 4), the flow is zero because permeability K is zero. A small amount of liquid water is present but not in continuous columns. Moisture movement effectively is by bound water diffusion driven by a gradient in moisture content, because vapor diffusion is negligible at these higher moisture contents. The liquid is reduced through adsorption by the cell wall at the liquid – bound water interface.

Equations 4 are used here to describe both gain and loss of water by capillary flow. As far as the author is aware, there are no published reports describing models of capillary uptake of water by wood. Though they presented data only for water loss, Spolek and Plumb (1981) state that a capillary pressure approach should apply equally well to penetration of wood by water. Extensive model trials for the case when the surface is wetter than the interior, as in wetting due to rain, yielded reasonable moisture distributions and average moisture content values. Thus eqs. 3–5 were used for wetting without further study.

Moisture diffusion within 10-h fuel sticks is treated as the isothermal combined diffusion of bound water and water vapor. Carlson and Gay (1980) noted that 10-h sticks exchange moisture isothermally, and a similar claim is advanced in the section on boundary conditions. The equation for isothermal diffusion of moisture is

$$[6]\qquad r\frac{\partial m}{\partial t} = \frac{\partial[rD(\partial m/\partial r)]}{\partial r}$$

where D is the moisture diffusivity (m^2·h^{-1}) obtained by summing the bound water diffusivity, D_b, and water vapor diffusivity, D_v. Thus D is written as

$$[7]\qquad D = D_b + D_v$$

where all three terms are on a volume of whole wood basis.

A more comprehensive treatment of diffusion in 10-h sticks would include a water vapor transport equation similar to eq. 6. Several wood-drying investigators have assumed, however, that the drying of wood below fiber saturation may be described satisfactorily with an overall diffusivity that combines the diffusivities associated with various transport mechanisms (Stamm 1964; Choong 1965; Siau 1995). Equation 7 is based on a similar, but much simplified, approach that is justifiable because D_v is a weak function of the ambient air humidity fraction, H, and hence of moisture fraction, m. This behavior is due to the weak dependence of the reciprocal slope of the sorption isotherm, dH/dm, on H (except at the extremes of H). The dependence of D_v on m is illustrated in Fig. 3, in which local values of D, D_b, and D_v are plotted for a stick temperature of 300 K. The curves are based on

Fig. 3. Moisture diffusivity as a function of local moisture content fraction at a stick temperature of 300 K. Solid line, combined bound water – water vapor diffusivity, D; short dashes, bound water diffusivity, D_b; long dashes, water vapor diffusivity, D_v. True diffusivities values are obtained by multiplying the values on the y axis by 10^{-6}.

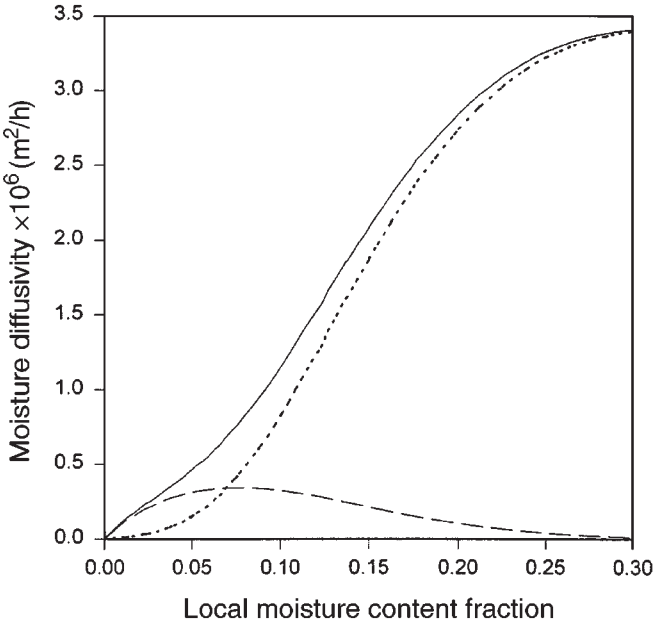

eqs. 7, B6, and B11. The contribution of vapor diffusion to the overall diffusion is significant for m smaller than 0.15, but becomes dominant below about 0.04. Thus, including vapor diffusion in the analysis should lead to more accurate moisture content predictions for hot, dry weather than only a bound water diffusion analysis would provide.

Boundary conditions

The energy balance at the stick surface ($r = a$, where a is the stick radius) is given by

$$[8]\qquad -k\left(\frac{\partial T}{\partial r}\right)+\frac{4B\varepsilon(T_{sk}+273.2)^3(T_s-T_{sk})}{\pi}+\frac{(Q_v+Q_w)G_v}{M_w}=\frac{fI_o(1-\alpha)}{\pi}+h_c(T_a-T_s)$$

where k is the stick thermal conductivity (377 $J\cdot m^{-1}\cdot h^{-1}\cdot K^{-1}$), B is the Stefan–Boltzmann constant (2.04×10^{-4} $J\cdot m^{-2}\cdot h^{-1}\cdot K^{-4}$), ε is the stick longwave emissivity (0.85), T_{sk} is the effective sky temperature (°C), T_s is the stick surface temperatue (°C), Q_v is the heat of vaporization of liquid water at temperature T_s ($J\cdot mol^{-1}$), Q_w is the differential heat of sorption ($J\cdot mol^{-1}$), G_v is the rate of water loss by evaporation or desorption ($kg\cdot m^{-2}\cdot h^{-1}$), M_w is the molecular weight of water (0.018 $kg\cdot mol^{-1}$), I_o is the solar constant (4.87×10^6 $J\cdot m^{-2}\cdot h^{-1}$), f is the fraction of solar constant received at the site, α is the stick surface albedo (0.6), h_c is the convective heat transfer coefficient (1.59×10^4 $J\cdot m^{-2}\cdot h^{-1}\cdot K^{-1}$), and T_a is the ambient air temperature (°C).

Terms on the left side of eq. 8 represent heat loss due to conduction away from the surface, longwave radiative cooling, and evaporation or desorption. Quantity G_v is positive for evaporation and desorption (Kreith and Sellers 1975). Terms on the right are heat gains owing to solar radiation and convective heating by the ambient air. The radiation terms are multiplied by $2/\pi$ to convert them to a stick surface basis. The stick emissivity and albedo are taken from Wengert (1966). It is assumed that only half the stick surface receives solar radiation and emits longwave radiation, regardless of the sun's position in the sky. On the other hand, the entire surface participates in conduction and convection. Terrestrial radiation seemingly should influence temperatures in the lower half of the stick, but field measurements with thermocouples located at the top, center, and bottom of standard 10-h sticks showed that temperatures are approximately constant regardless of stick moisture content or intensity of insolation. This result was observed repeatedly and subsequently was suggested by model calculations. Thus, stick temperature is computed from eq. 8 with the conduction term set to zero. Cloud cover and incoming longwave radiation are not considered explicitly in this simple model, but the effective sky temperature depends on time of day and is used as a model-tuning parameter. When the solar flux is nonzero, T_{sk} is set to 6°C; when the flux is zero, T_{sk} is set to 3°C. These values are found at levels between 1 and 2 km in the U.S. standard atmosphere (Hess 1959); whether these temperatures actually determine radiative cooling of the stick is not known.

Convective heat transfer coefficient, h_c, also is used as a model-tuning parameter and is taken to be constant. This approximation conflicts with heat transfer theory in which h_c is a function of the surrounding fluid, stick diameter, and wind speed. In forced convection, the constant, 1.59×10^4 $J\cdot m^{-2}\cdot h^{-1}\cdot K^{-1}$, corresponds to a wind flow of 0.056 $km\cdot h^{-1}$ (0.035 $mi\cdot h^{-1}$) around a stick 1.27 cm in diameter. This value for h_c is essentially the calm-air value of 1.6×10^4 $J\cdot m^{-2}\cdot h^{-1}\cdot K^{-1}$ reported by Siau (1995) and is slightly smaller than the free convection value of 2.2×10^4 $J\cdot m^{-2}\cdot h^{-1}\cdot K^{-1}$ for a 5°C temperature difference (Kreith 1967). Thus, the stick is exposed in essentially calm air, according to the tuned model. Clearly, the fraction of any given 24-h day during which this result will apply can range from 0 to 1. The atmosphere near the ground can be calm during the day and often is stable at night. Wind may produce an effect on the moisture-exchange rate of 10-h sticks only when free water covers the surface after rainfall, dew, or fog formation. It is for this reason that wind speed and direction were bypassed as weather inputs during model development. An additional argument supporting the small value of h_c is that, in the case of a crosswind, only the most upwind stick is fully exposed; the remaining three sticks are exposed only to the wake of their nearest upwind neighbor. Kreith (1967) points out that for aligned or staggered bundles of cylindrical tubes, the heat transfer coefficients in turbulent crossflow increase for the second and subsequent rows of tubes but decrease for laminar flow. As three of the four dowels making up the stick array are partially shielded when the wind blows, a small "effective" value of h_c seems plausible. Finally, the model-generated Biot number (or conduction Nusselt number), 0.27 (15 900 × 0.0064/377), indicates that the internal conductance is almost four times larger than the external conductance involving h_c (Schneider 1955). This result is

consistent with observations in this study and in the study of Carlson and Gay (1980) that temperature gradients in 10-h sticks are not large.

Stick surface temperature, T_s, is obtained from eq. 8 rewritten in the form

$$[9] \quad \frac{4B\varepsilon(T_{sk} + 273.2)^3(T_s - T_{sk})}{\pi} + h_v(T_a - T_s) = \frac{fI_o(1-\alpha)}{\pi} + h_c(T_a - T_s)$$

where h_v is a heat transfer coefficient ($J \cdot m^{-2} \cdot h^{-1} \cdot K^{-1}$) associated with vapor exchange between the stick and atmosphere given by

$$[10] \quad h_v = \frac{0.622 h_c (Pr/Sc)^{0.667} Q_v A}{c_a M_w}$$

and where 0.622 is the molecular weight ratio of water to air and c_a is the constant-pressure specific heat of air, 1005 $J \cdot kg^{-1} \cdot K^{-1}$. The Prandtl number, Pr, is assigned a value of 0.7, and the Schmidt number, Sc, taken from Kreith (1967), is 0.58. Quantity A is the psychrometric constant and, according to tables developed by Environment Canada (1976), has the value 0.000 772 $°C^{-1}$ when a psychrometer (or 10-h stick; see discussion leading to eq. 20) is nonventilated. A nonventilated psychrometer is defined in the Canadian work as "a psychrometer in which the natural movement of air is relied upon for ventilation." Equation 10 is developed in Appendix C. Coefficient h_v is set to zero during rainfall on the assumption that vapor transfer is zero.

The amount of water on the stick surface is affected by rainfall, condensation, and evaporation. It is assumed that the amount of rain falling between weather observations can be interpreted as an average over a 1-h interval, and that the surface moisture content fraction, m_s, increases linearly with time during the interval. For an observation interval immediately following an interval with no rain, this increase is calculated from one of the equations:

$$[11a] \quad dm_s = 0.8(1 - e^{-10R})\, dt$$

$$[11b] \quad dm_s = 0.12(1 - e^{-10R})\, dt$$

where dt is the computational timestep (a small fraction of the interval between weather observations). Quantity R, constant within the current interval, indicates the rainfall amount (mm) captured by the stick surface and is determined by multiplying the rainfall on an area-of-ground basis by the ratio of the stick planform area to its surface area, $1/\pi$. Thus, the amount of rain captured by the stick during an hourly rainfall of 2 mm is $2/\pi$ mm. Equation 11a is used when the relative humidity is either increasing or unchanged from the previous observation; it suggests that, during intervals of constant or increasing humidity, the maximum increase in m_s occurs when the captured rainfall is about 0.4 mm and that heavier initial rain does not increase the effectiveness of wetting the stick surface. Equation 11b is used when the relative humidity is decreasing. It is assumed that evaporation slows the increase in m_s owing to a decrease in humidity during an interval when rain occurs. Such decreases may be seen in field data because rain, in many instances, does not fall during an entire interval.

Fig. 4. Changes in stick average moisture content fraction versus hourly captured rainfall (dt = 1 h) during field experiments in Burnsville, N.C. (circles), and Mio, Mich. (triangles). Solid symbols, initial moisture fraction smaller than 0.4; open symbols, initial fraction greater than 0.4.

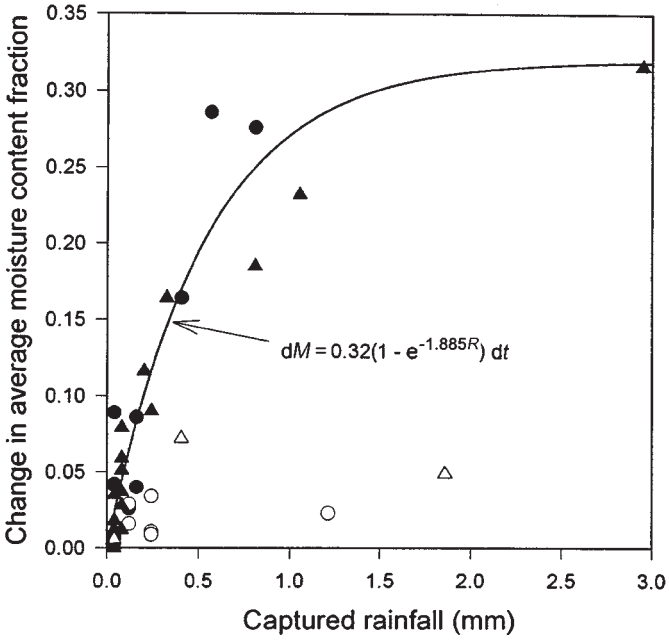

The form of eqs. 11 was determined from examination of field data. Figure 4 shows the change in stick-average moisture content fraction, dM, plotted against captured hourly rainfall, R, for data collected in Burnsville, N.C., and in Mio, Mich. These experiments are described later. Although observations are scarce for R >1 mm, the equation of a visually fitted curve through the data for M <0.4 is

$$[12] \quad dM = 0.32(1 - e^{-1.885R})\, dt$$

where dt is 1 h. This equation involving the average stick moisture fraction suggested that similar equations might describe changes in the surface moisture fraction, dm_s. Equations 11 are of the same form as eq. 12, but their constants were determined by model trials. These equations are applied only to the first observation interval during a precipitation event. The data in Fig. 4 for M >0.4 indicated that dm_s should be small for the second and succeeding intervals. Thus, when rain falls during two or more consecutive observation intervals, the amount captured is accumulated with a running total of R denoted by Z. Within any interval (excluding the first), dm_s increases linearly with time according to

$$[13] \quad dm_s = 0.007Z\, dt$$

until m_s equals 0.6, after which value all additional rainfall intercepted by the surface is assumed to run off. Thus, the maximum average moisture content fraction the stick can achieve is limited to 0.6. Maximum stick moisture fractions of 0.6 were observed by Deeming (1983) and by the author

during field experiments discussed later. When the rain ceases for an entire observation interval, Z is reset to zero.

After numerous model runs, it was realized that the foregoing method of computing m_s leads to an acceptable prediction of the increase in stick average moisture fraction during gentle rains but that severe underpredictions occur during periods of heavy rain. Thus, distinction between a rainfall and a rainstorm is made in the model. During any observation interval for which R exceeds 0.365 mm, a rainstorm is declared and m_s immediately is set to 0.6. It is postulated that the water film surrounding the stick develops to such an extent that a fixed amount of water, 1.72 g, is added to the stick externally (it is further assumed that a thinner film of negligible weight develops during gentle rain because of sufficient time for absorption of potential film water by the stick). Rainstorm data from the field experiments (Fig. 4) suggested that R = 0.365 mm raises the average moisture content fraction by about 0.16; however, to account for storms with heavier rain, R in the model is fixed at a value of 0.45 mm, increasing the moisture fraction change to 0.183. If it is also assumed that 62% of this water is absorbed by the stick, the increment in stick moisture fraction due to the external film is 0.069. In the model, this increment is added to the average moisture fraction computed from capillarity and diffusion considerations with m_s equal to 0.6. Inherent in this approach is the possible overprediction of average moisture fraction when R for a storm is smaller than 0.45 mm. It is noted that cases can occur for which the average moisture fraction is near 0.6 and then a storm occurs. Conceivably, the stick-average moisture content could exceed 0.6 due to the surface film, but this possibility is not treated in the model. In no case does the modeled average moisture content fraction exceed 0.6; all water from additional precipitation is assumed to run off.

When rainfall is absent, condensation (collection of dew on the stick surface) or evaporation may occur, but contact with fog is not considered in the model. It is assumed that the effects of dew and fog on stick moisture fraction are identical. Occasionally after rain, especially during early morning hours, air temperature and relative humidity become static, neither condensation nor evaporation occurs, and model values of m_s do not change. Such periods are referred to as periods of stagnation and can last up to 8 h. In the absence of stagnation, evaporation occurs during drying after rain and continues until m_s becomes smaller than m_{fsp}. Two kinds of evaporation occur in the model. The first is evaporation after rainfall and is discussed below (see discussion leading to eq. 17). The second kind of evaporation is that following one or more successive weather observation intervals during which a rainstorm occurs. If the storm takes place during evening or early morning hours, environmental conditions often are not conducive to evaporation, there is little or no change in stick moisture content, and the stick surface relative humidity fraction stays at 0.99. During this time, addition of the moisture fraction increment 0.069 to the average moisture fraction obtained from capillarity and diffusion calculations is continued, so the net moisture fraction change is small. Evaporation begins after a storm period only when the humidity fraction at the stick surface drops below 0.99. In this case, it is assumed that all water in the external film quickly disappears, resulting in a sharp decrease in predicted moisture fraction, because the moisture increment of 0.069 is no longer added to the average value computed from capillarity and diffusion.

Condensation and evaporation following rainfall (in the model) primarily depend on water vapor pressure differences between the air and stick surface and on stick surface temperature, T_s. Condensation often appears in the early morning hours before sunrise. In the model, condensation is triggered (regardless of the value of m_s) when T_s equals or is exceeded by T_d, the ambient air dewpoint temperature (taken from Skaar 1988). This process usually continues until just after sunrise when T_s becomes greater than T_d. In initial trials, changes in m_s due to condensation or evaporation were described by

$$[14] \quad dm_s = -2E_p\, dt$$

where E_p is the rate of surface moisture fraction change due to vapor pressure differences (the vapor pressure effect), and is written as

$$[15] \quad E_p = \left[\frac{0.662 h_c (Pr/Sc)^{0.667}}{\rho c_a P_b a}\right](p_s - P_d)$$

where 0.622 is the molecular weight ratio of water to air, Pr is the Prandtl number (0.7), Sc is the Schmidt number (0.58), c_a is the constant-pressure specific heat of air (1005 $J \cdot kg^{-1} \cdot K^{-1}$), P_b is the site-dependent barometric pressure ($kg \cdot m^{-1} \cdot h^{-2}$), a is the 10-h stick radius (0.0064 m), p_s is the vapor pressure at the stick surface ($kg \cdot m^{-1} \cdot h^{-2}$), and P_d is the saturation vapor pressure of water at temperature T_d, ($kg \cdot m^{-1} \cdot h^{-2}$). Equation 15 is based on heat and mass transfer similarity (Kreith 1967) and is developed in Appendix C.

Use of eqs. 14 and 15 in model trials demonstrated that surface evaporation rates were slow, resulting in an unrealistically large uptake of water within the stick by capillarity. It was postulated that, in the case of evaporation, an additional depletion of the surface water film occurs because of flow into fiber cavities within a thin layer of wood just below the surface. An expression for the rate of surface moisture fraction change due to this inward flow (or capillary effect) is derived in Appendix A as

$$[16] \quad E_c = \frac{\pi s r_c^2}{16 \nu L \rho a^2}$$

where r_c is the fiber cavity radius (9.2×10^{-6} m), L the stick length (0.5 m), and ν is from eq. 5. Thus, for evaporation following condensation or gentle rain, eq. 14 becomes

$$[17] \quad dm_s = -(2E_p + E_c)\, dt$$

The inward flowing water described by eq. 16 is a source of internal moisture but is not accounted for in eqs. 4.

Brief numerical experiments were conducted to check the effect of changes in P_b from eq. 15 on predicted stick moisture fraction. A 15% reduction in P_b slightly increased the evaporation rate and reduced the stick average moisture content fraction by 0.007 or less. It was deemed unnecessary to include varying P_b as a regular weather input to the model.

The final boundary condition considered is that of bound water sorption. A factor complicating the description of moisture transport below m_{fsp} is hysteresis in equilibrium

moisture content values following adsorption and desorption. This effect can cause significant moisture fraction differences in model calculations. Other problems are that data on sorption of water vapor by ponderosa pine wood are not available and that sorption hysteresis is not well understood or described mathematically (Peralta 1995). Thus, the sorption isotherm of Hart (1977) was fitted to adsorption and desorption data of Blackmarr (1971) for loblolly pine (*Pinus taeda* L.) wood at a reference temperature of 26.7°C. These two isotherms then were averaged to produce a single isotherm, thereby eliminating discontinuities in equilibrium moisture fraction caused by hysteresis. A similar averaging procedure was used by Peralta and Skaar (1993). Moisture fraction calculations were corrected for temperatures other than the reference value with the Clausius–Clapeyron method suggested by Skaar (1988). These manipulations lead to a fractional equilibrium moisture content, m_e, given by

$$[18] \quad m_e = U[-\ln(1 - H_s)]^u$$

where H_s is the fractional relative humidity at the stick surface and U and u are written as

$$[19a] \quad U = 0.1617 - 0.001\,419\,T_s$$

$$[19b] \quad u = 0.4657 - 0.003\,578\,T_s$$

Equation 18 shows that m_e is undetermined when H_s equals unity; in this case H_s is set to 0.99.

Evaluation of p_s and H_s in eqs. 15 and 18 is accomplished with a procedure due to Hart (1977) who proposed that a wood surface with m_s less than m_{fsp} acts like a wet-bulb thermometer and that the water vapor pressure at the surface, p_s, can be computed from the psychrometric equation if the surface temperature, T_s, is known. In this equation, p_s and T_s replace values of vapor pressure and temperature evaluated at the wet-bulb temperature. A study supporting this approach is presented by Rosen (1982). The wind speed implied in the model, 0.056 km·h^{-1}, is much smaller than 3.66 km·h^{-1}, the wind speed required for efficient operation of a wet-bulb thermometer. Thus, a psychrometer constant appropriate for a nonventilated wet bulb (or 10-h stick) is used in the model (Environment Canada 1976). Calculated p_s values appear reasonable. With an estimate of T_s available from eqs. 9 and 10, p_s can be computed from

$$[20] \quad p_s = H_a P_a + P_b A(T_a - T_s)\left(\frac{Q_v}{Q_v + Q_w}\right)$$

where H_a is the fractional relative humidity of ambient air, T_a is the air temperature (°C), P_a is the saturation vapor pressure at T_a (kg·m^{-1}·h^{-2}), and A is the "no ventilation" psychrometric constant (0.000 772 °C^{-1}). The ratio $Q_v/(Q_v + Q_w)$ corrects A for the latent heat involved in vaporization of bound water or condensation of vapor to bound water. Thus, H_s is obtained from

$$[21] \quad H_s = \frac{p_s}{P_s}$$

where P_s is the saturation vapor pressure of water (kg·m^{-1}·h^{-2}) at T_s.

A value of m_s is computed from the surface water balance written as

$$[22] \quad -D_s\left(\frac{\partial m}{\partial r}\right) = h_m(m_s - m_e)$$

where D_s is the moisture diffusivity at the stick surface (m^2·h^{-1}) and h_m is the surface emission coefficient (m·h^{-1}). Several approaches to evaluation of h_m have been used by wood drying researchers (Choong and Skaar 1972; Avramidis and Siau 1987; Moren et al. 1992; Gong and Plumb 1994), but no proven method exists for quantifying h_m when wood contains only bound water and water vapor. Equation 20, from the Hart (1977) theory, eliminates this problem because it is an equilibrium relationship. This implies that rates of heat and moisture transfer at the surface are large relative to rates of change in H_a, T_a, and insolation fI_o (fortunately, a realistic circumstance in this modeling effort) and that m_s equals m_e in the limit of infinite h_m. An effectively infinite value of 25 m·h^{-1} is assigned to h_m for desorption. On the other hand, the constant value of h_m for adsorption is much smaller; h_m was used as a model-tuning parameter along with h_c and T_{sk}. The value chosen, 0.0003 m·h^{-1}, lies within the range of experimental h_m values listed by Siau (1995) and leads to reasonable estimates of m_s during adsorption. The manipulation of h_m for adsorption and desorption to mimic effects of hysteresis on D_s does not describe the physical processes but produces an adsorption slower than desorption in agreement with field observations and with results from laboratory experiments on diffusion of bound water in wood (Comstock 1963).

The value of m_s is obtained by expressing eq. 22 in finite-difference form. This leads to

$$[23] \quad -D_s(m_s - m_2) = h_m\Delta r(m_s - m_e)$$

where m_2 is the moisture fraction at the numerical calculation node just inside the stick surface. This node and the surface node are separated by distance Δr. A surface mass transfer Biot number is defined as

$$[24] \quad \mathrm{Bi} = \frac{h_m\Delta r}{D_s}$$

and leads to

$$[25] \quad m_s = \frac{m_2 + m_e\mathrm{Bi}}{1 + \mathrm{Bi}}$$

The desorption h_m value is so much larger than that for adsorption that Bi for desorption usually exceeds the adsorption Bi by a factor of 10 or more. Thus, m_s for desorption effectively equals m_e; for adsorption, m_s lags m_e slightly.

After computation of m_s with one of the boundary conditions on m discussed above, the liquid saturation at the surface, S_s, is obtained from eq. 2 when m_s exceeds m_{fsp}. Otherwise, S_s is set to zero.

Numerical procedures

Model calculations begin with initialization of 10-h stick properties and fixed weather variables. Initial conditions involve uniform distributions of stick temperature and moisture content fraction. Calculations continue with input of

new values for air temperature and relative humidity, solar pyranometer voltage reading (later converted to a fraction of the solar constant), and rainfall amount since the previous weather observation. It is assumed that, between weather observations (a 1-h observation interval is suitable for 10-h sticks), all four input variables change from old to new values in a linear manner. The stick surface temperature is computed and then used to estimate moisture diffusivity and sorption equilibrium parameters. Calculation of the moisture fraction boundary condition begins with a test for rainfall. The occurrence of rain pre-empts all other surface processes. Gentle rainfall occurs when the amount captured by the stick is less than the storm-transition value of 0.365 mm. The stick surface moisture content is a function of time, and the average moisture content fraction is determined by capillary and diffusional flow. On the other hand, a rainstorm occurs when the captured precipitation exceeds the transition value. In this case, the surface moisture fraction immediately jumps to 0.6, and a surface film boosts the average moisture content fraction computed from capillarity and diffusion considerations by an additional fixed amount, 0.069.

If rain has not fallen, the stick surface and dewpoint temperatures are compared. A lower surface temperature triggers condensation, and other surface processes are excluded. If the surface temperature is larger than the dewpoint temperature and the current surface moisture fraction exceeds the fiber saturation point, either condensation or evaporation can occur, depending upon vapor pressures at the surface and in the ambient air. Immediately following a precipitation period during which a storm occurred, the surface film does not begin to evaporate until the relative humidity fraction at the stick surface falls below 0.99. All subsequent evaporation effects are calculated from the vapor-pressure difference. If the surface moisture fraction is smaller than the fiber saturation point, sorption occurs. This process is desorption if the current surface moisture fraction exceeds the equilibrium value; if the current value is smaller, adsorption occurs; and if the values are equal, no sorption takes place at the surface.

With the new estimates of surface temperature, saturation, and moisture fraction, the model calculates new values of these variables along the stick radius (20 interior nodes) by explicit finite-difference methods (Patankar 1980). For the 10-h stick, a computational time step of 1 min works well, because interior temperatures are set equal to the surface value (the stick is always isothermal). If this were not so, a much smaller time step would be required to insure computational stability. New temperatures are determined first because of the rapid heat transfer; liquid saturation values are computed next and are followed by diffusion calculations when these are required. If all stick locations are at saturation levels such that the permeability is nonzero ($S > S_c/4$), there is no diffusion because there is no gradient in bound water. Thus, flow is by capillarity and the diffusion calculations are bypassed. On the other hand, if at any point in the stick some liquid remains but the permeability is zero ($0 < S < S_c/4$), the flow of liquid must be by diffusion and the calculations are done. This computation is artificial if the flow is to an adjacent location that contains a smaller amount of liquid water, because liquid water, in fact, does not move by diffusion. Thus, artificial flow can occur only if a gradient in bound water content is present in an outer region of the stick. The diffusion calculation is realistic, however, if the flow is to a region where no free water is present. In this case, the liquid can be adsorbed within the cell wall.

The moisture diffusivity is updated at convenient times between successive weather observations using current values of stick moisture fraction and temperature. Average moisture content fraction of the stick is obtained by integration using Simpson's rule. Upon completion of interval calculations, newly computed variable values are reset as old values, time counters are reset, and a new interval is initiated with new weather input.

Field studies

Experiments

Field experiments involving collection of weather data and 10-h stick weights were carried out at Burnsville, N.C. (35°55′N, 82°18′W; 858 m a.s.l.), during August 1993, and at Mio, Mich. (44°39′N, 84°07′W; 312 m a.s.l.), during September 1993. The Burnsville site was an open field with a thin cover of mown stubble grass; sticks were located 30 m from the nearest building. The Mio site was a grass lawn with shrubbery and small trees at the eastern edge about 15 m from the sticks; the nearest building was 25 m away. Five sets of randomly selected standard 10-h fuel sticks were set out at each site according to accepted guidelines (Finklin and Fischer 1990). The arrays were placed side by side on a rack and were 10 cm apart. A RAWS also was erected at each site but served only as backup to weather data collected manually with a sling psychrometer (air temperature and relative humidity). Although use of the psychrometer was more laborious, the method provided protection from a possible RAWS malfunction during these initial experiments. Insolation was measured with a solar pyranometer and rainfall with a plastic gauge readable to the nearest 0.25 mm. Stick temperature was obtained from voltmeter readings for three type K thermocouples 0.13 mm in diameter located near the top, center, and bottom of a single dowel within an additional array of sticks. Stick weight was measured with a sheltered portable platform balance readable to the nearest 0.1 g. The data were collected hourly by two observers alternating shifts around the clock. Table 1 summarizes daily extremes in weather at the two sites. Data from each site were used to calibrate the model and then plots were made of stick moisture content fraction (an average of the five arrays) versus time.

These experiments also provided information about variation among sets of sticks exposed to the same weather. Differences among weight readings for the five arrays at each site indicate that, below a moisture fraction of 0.15 and in the absence of rain, the individual arrays track one another within 0.02; between 0.15 and 0.3, the sticks track within 0.04; and above 0.3, the arrays can differ in fractional moisture content by as much as 0.1. The differences above 0.3 are easily explained by the approximate weights obtained under rainy conditions (sticks were not blotted or shaken prior to weighing); the differences below 0.3 are caused by measurement error and variation (natural and introduced during manufacture) among stick arrays. These results were obtained

Table 1. Extremes in weather recorded daily at sites of two 10-h fuel stick moisture content experiments during the summer of 1993.

Month and day	Air temperature (°C)		Air relative humidity (fraction)		Maximum fraction of solar constant	Total rainfall amount (mm)
	Minimum	Maximum	Minimum	Maximum		
Burnsville, N.C.						
Aug. 10	17	24	0.55	0.85	0.21	0.0
Aug. 11	12	24	0.57	0.94	0.50	0.0
Aug. 12	15	24	0.63	1.00	0.42	0.9
Aug. 13	17	24	0.71	1.00	0.27	10.4
Aug. 14	18	28	0.60	1.00	0.72	0.0
Aug. 15	17	29	0.48	0.95	0.66	0.0
Aug. 16	14	31	0.44	1.00	0.65	0.0
Aug. 17	17	31	0.42	0.95	0.78	0.0
Aug. 18	17	30	0.46	0.95	0.70	0.0
Aug. 19	16	29	0.51	0.95	0.67	0.1
Aug. 20	17	31	0.49	0.95	0.62	2.5
Aug. 21	17	28	0.51	1.00	0.66	0.0
Aug. 22	14	27	0.58	0.95	0.64	0.0
Aug. 23	16	19	0.86	0.95	0.05	0.0
Mio, Mich.						
Sept. 11	9	11	0.78	0.80	0.00	0.0
Sept. 12	9	18	0.64	0.87	0.29	0.0
Sept. 13	18	26	0.64	1.00	0.34	9.3
Sept. 14	11	23	0.73	0.98	0.13	8.9
Sept. 15	4	15	0.51	0.97	0.60	1.8
Sept. 16	3	15	0.56	1.00	0.47	0.0
Sept. 17	4	17	0.56	0.96	0.52	0.0
Sept. 18	8	22	0.41	0.93	0.59	0.8
Sept. 19	0	17	0.40	0.95	0.53	0.0
Sept. 20	4	16	0.54	0.96	0.59	0.3
Sept. 21	8	17	0.49	0.97	0.36	0.3
Sept. 22	3	18	0.51	1.00	0.23	1.3
Sept. 23	6	17	0.46	0.98	0.53	0.4
Sept. 24	1	6	0.92	1.00	0.02	0.0

for conditions as close to "ideal" as possible and, therefore, define a level of precision that model predictions should achieve if they are to represent "best possible" estimates.

In June and July of 1996, field measurements were conducted by personnel from the Fire Management Office of the Lolo National Forest, Lolo, Mont., to obtain independent data for testing model predictions. Data involving triplicate observations were collected from June 10 to June 18. Three arrays of new standard 10-h sticks were set out at the NFDRS station in Missoula, Mont. (46°52′N, 113°59′W; 982 m a.s.l.), according to recommendations of Finklin and Fischer (1990) and then allowed to condition for 3 days. The sticks were located about 45 m from the nearest building. Several times a day they were weighed to the nearest 0.5 g with a hand-held Williams scale (Finklin and Fischer 1990). Moisture content was determined by assuming that each array weighed 100 g when oven dry. The three moisture contents were averaged to determine observed values for comparison with model predictions. A RAWS recorded hourly readings of air temperature and relative humidity, precipitation, and insolation. Table 2 presents a summary of the daily extremes in these variables at the Missoula site. As in the Burnsville and Mio data, air temperature did not exceed 31°C. On the other hand, relative humidity fraction dropped to a minimum of 0.2, causing the fractional moisture content to dip below 0.1.

Predicted versus observed

Figures 5 and 6 show comparisons of predicted and observed moisture content fraction over the duration of the experiments for Burnsville and Mio, respectively. Agreement is generally within the bounds of variation described earlier, but notable exceptions occur in the Mio data (collected when conditions were relatively cool and wet). In Fig. 5, the rise and fall of moisture fraction due to gentle rain on August 13 is predicted well except for the spike to 0.6 due to a brief rainstorm just before noon. The sharp increase in moisture fraction due to a rainstorm on August 20 is predicted well; the small decrease immediately following the storm is not calculated as such in the model but as an increase due to condensation on the stick surface. The rapid fall in moisture fraction following precipitation is predicted well for both events. Moisture recovery following adsorption is both under- and over-predicted. In Fig. 6, the moisture fraction increase resulting from gentle rain after 06:00 on September 14 is overpredicted by 0.05 to 0.1, but the increase due to an

Table 2. Extremes in weather recorded daily during a 10-h fuel stick moisture content experiment in Missoula, Mont., in June 1996.

Month and day	Air temperature (°C)		Air relative humidity (fraction)		Maximum fraction of solar constant	Total rainfall amount (mm)
	Minimum	Maximum	Minimum	Maximum		
June 10	12	27	0.25	0.61	0.67	0.0
June 11	10	24	0.23	0.69	0.73	0.0
June 12	4	27	0.27	0.96	0.68	0.0
June 13	6	31	0.20	0.92	0.67	0.0
June 14	13	28	0.29	0.74	0.68	0.0
June 15	11	31	0.26	0.97	0.72	3.3
June 16	10	30	0.37	1.00	0.66	1.3
June 17	7	22	0.35	0.94	0.60	3.6
June 18	6	12	0.41	0.92	0.52	0.0

Fig. 5. Burnsville, N.C., moisture content fraction (average of five arrays of 10-h sticks) as observed (broken line) and predicted (solid line) versus time expressed as calendar date.

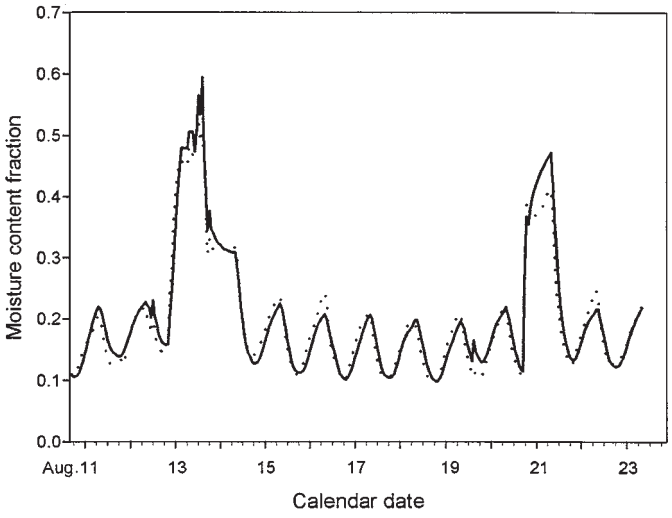

Fig. 6. Mio, Mich., moisture content fraction (average of five arrays of 10-h sticks) as observed (broken line) and predicted (solid line) versus time expressed as calendar date.

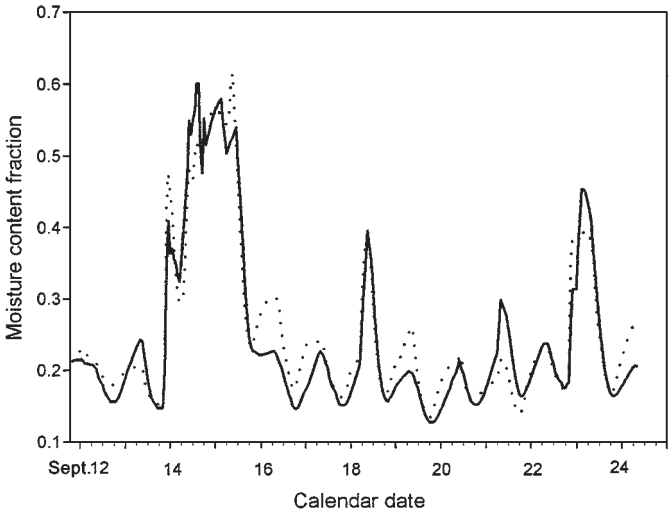

earlier rainstorm after 18:00 on September 13 is underpredicted by about 0.07. The overprediction of 0.085 on September 21 may be partly due to faulty rainfall data (and partly due to overestimated adsorption). For a period of several hours, traces of rain were observed with the gauge, but none were recorded by the RAWS. It is likely that the reading from the gauge was in error. Such uncertainties in rainfall data must be eliminated because a misprediction of 0.085 when the actual moisture fraction is 0.22 is of little practical value. The rainfall after 18:00 on September 22, with an amount close to the storm-transition value, perhaps should have been classified as a storm which would explain the model's underestimate of 0.07; this is followed immediately by a period of overprediction by 0.07. The decline in moisture content fraction after each of the three major precipitation events is described well, but peak moisture fractions during early morning hours are generally poorly predicted. Moisture recovery by adsorption and (or) condensation is both underpredicted (September 17 and 20) and overpredicted (September 13 and 21). In all of these cases, dew was not observed on the sticks and was not predicted by the model. On the mornings of September 16, 19, and 24, dew was observed but not predicted and adsorption rates were underpredicted. The underpredictions on September 16 and 24, however, may be partly explained by the presence of fog. The effects of fog are not considered in the model.

Figure 7 shows a comparison of the 10-h stick fractional moisture content observations made independently by Lolo National Forest personnel and the corresponding hourly predictions. The differences between observation and prediction usually fall within the range in variability found in the Burnsville and Mio data, but a generally slow response is indicated for moisture fractions between 0.05 and 0.15. The model slightly overpredicts the smaller moisture fraction values and underpredicts the recovery during early morning hours. The predicted increase and decrease in moisture fraction during and after rain between June 15 and June 17 is in good agreement with the data.

The variability exhibited in the three data sets described above may be explained by variation among batches of 10-h sticks or by differences in experimental methods. Clearly, further tests are needed. The comparisons indicate that the model performs better in dry than in wet conditions. This result is expected, especially in view of the crude treatment of

Fig. 7. Missoula, Mont., moisture content fraction (average of three arrays of 10-h sticks) as observed (plus signs) and predicted (solid line) versus time expressed as 1996 calendar date.

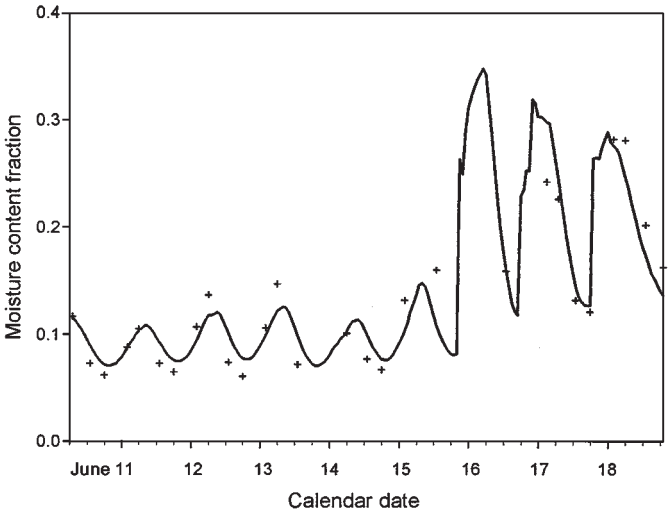

rainfall and water film dynamics. The generally good agreement in Figs. 5 and 6 is expected because the model was calibrated with the field data.

Application

With a small amount of additional research, the 10-h moisture content prediction model presented earlier may be applied to wood dowels of any reasonable size. An obvious application is to surrogate fuels in the NFDRS. Another possibility is the near-real-time prediction of wood moisture content for users in agricultural or forestry activities (for example, prescribed burning). Modification of the stick radius, computational time step, weather observation interval, and tuning parameters would be required to apply the model to dowels of differing diameter. The additional research needed is on the response of these different dowels to precipitation. Use of the formulation for 10-h sticks within models for 1-, 100-, and 1000-h fuels undoubtedly would be faulty, owing to its empirical basis and upper limit on average moisture content of 60%. The 1-h stick, for example, may exhibit average moisture contents during rain approaching 100% because of its smaller radius. Field experiments combined with a theory of runoff would be needed to make the model generally applicable in rainy weather.

Although the comparisons in Figs. 5–7 are encouraging, model predictions should be checked with additional independent data collected in extremely hot and dry weather. Another question concerns whether the response to wind is adequately modeled under wet conditions. Results to date suggest that the convective heat transfer coefficient now in use provides an adequate description. In addition, the tendency toward moisture content underprediction during early morning hours may reflect either an incomplete formulation of surface transfer or an incorrect description of the temperature effect on adsorption. Also, the criterion indicating dew formation may require improvement. There are other uncertainties about the need to include the freezing of water and to distinguish between dew and fog. Studies are being conducted to answer these questions and identify other weaknesses.

Summary

Estimates of surrogate fuel moisture content in the NFDRS are rough approximations because weather information is not supplied with sufficient frequency to allow reliable prediction of moisture transport in the fuel. A new prediction scheme for 10-h fuel sticks utilizing frequent weather observations is described. Use of the model is straightforward, as the weather inputs are limited to air temperature and relative humidity, solar radiation flux, and rainfall amount. Equations describing heat and moisture transfer at the surface and within the stick are solved to obtain estimates of stick temperature and average moisture content.

Field experiments conducted in the summer of 1993 provided stick weight and temperature data to guide model development. Comparisons of predicted and observed moisture content indicate differences of about the same magnitude as the differences among weights of five arrays of 10-h sticks weighed individually in the field. This agreement is expected, however, as the model was calibrated with the field data.

Daily stick moisture content measurements conducted in 1996 by personnel of the Lolo National Forest provided an independent test of the model's prediction capability. Predictions were not always within the bounds of acceptable agreement identified in the 1993 studies and indicate a need for additional tests.

In the absence of rainfall, the model easily may be adapted to dowels of differing size. A potential application is for predicting moisture contents of the various fuel classes in the NFDRS, but further research is needed to generalize rainfall in the model. Studies are underway to identify model limitations and improve predictions.

Acknowledgements

Discussions with Don Latham of the Intermountain Fire Sciences Laboratory contributed significantly to completion of this research. The support of Paul Sopko, also of the Laboratory, during collection and analysis of the field data is gratefully acknowledged. Thanks are extended to Howard Roose, Fire Management Officer on the Lolo National Forest, for providing weather and 10-h stick moisture content data to the author for use in this study.

References

Avramidis, S., and Siau, J.F. 1987. An investigation of the external and internal resistance to moisture diffusion in wood. Wood Sci. Technol. **21**: 249–256.

Beall, F.C. 1968. Specific heat of wood—further research required to obtain meaningful data. USDA For. Serv. Res. Note FPL-0184.

Blackmarr, W.H. 1971. Equilibrium moisture content of common fuels found in southeastern forests. USDA For. Serv. Res. Pap. SE-74.

Bradshaw, L.S., Deeming, J.E., Burgan, R.E., and Cohen, J.D. 1983. The 1978 National Fire Danger Rating System: technical documentation. USDA For. Serv. Gen. Tech. Rep. INT–169.

Burgan, R.E. 1988. 1988 revisions to the 1978 National Fire Danger Rating System. USDA For. Serv. Res. Pap. SE-273.

Carlson, J.N., and Gay, L.W. 1980. The energy budget of a fuel moisture stick. *In* Proceedings of the 6th Conference on Fire and Forest Meteorology, 22–24 Apr. 1980, Seattle, Wash. Society of American Foresters, Washington, D.C. pp. 246–255.

Choong, E.T. 1965. Diffusion coefficients of softwoods by steady-state and theoretical methods. For. Prod. J. **15**(11): 21–27.

Choong, E.T., and Skaar, C. 1972. Diffusivity and surface emissivity in wood drying. Wood Fiber, **4**(2): 80–86.

Comstock, G.L. 1963. Moisture diffusion coefficients in wood as calculated from adsorption, desorption, and steady state data. For. Prod. J. **13**(3): 97–103.

Comstock, G.L. 1970. Directional permeability of softwoods. Wood Fiber, **1**(4): 283–289.

Cramer, O.P. 1961. Predicting moisture content of fuel-moisture-indicator sticks in the Pacific Northwest. USDA For. Serv. Res. Pap. PNW-41.

Deeming, J.E. 1983. A preliminary model for calculating the ten-hour timelag fuel moisture from hourly weather data. Presented at the 7th Conference on Fire and Forest Meteorology, 25–28 Apr. 1983, Fort Collins, Colo. Unpublished manuscript. USDA Forest Service, Fire Sciences Laboratory, Rocky Mountain Research Station, Missoula, Mont.

Deeming, J.E., Burgan, R.E., and Cohen, J.D. 1977. The National Fire-Danger Rating System—1978. USDA For. Serv. Gen. Tech. Rep. INT-39.

Environment Canada. 1976. Psychrometric tables. Book 1. Atmospheric Environment Service, Downsview, Ont.

Finklin, A.I., and Fischer, W.C. 1990. Weather station handbook—an interagency guide for wildland managers. National Wildfire Coordinating Group, Boise Interagency Fire Center, Boise, Idaho. Publ. NFES 2140.

USDA Forest Products Laboratory. 1987. Wood handbook: wood as an engineering material. U.S. Dep. Agric. Agric. Handb. 72.

Fosberg, M.A. 1977. Forecasting the 10-hour timelag fuel moisture. USDA For. Serv. Res. Pap. RM-187.

Fosberg, M.A., and Deeming, J.E. 1971. Derivation of the 1- and 10-hour timelag fuel moisture calculations for fire-danger rating. USDA For. Serv. Res. Note RM-207.

Gisborne, H.T. 1933. The wood cylinder method of measuring forest inflammability. J. For. **31**: 673–679.

Gong, L., and Plumb, O.A. 1994. The effect of heterogeneity on wood drying, part I: model development and predictions. Drying Technol. **12**: 1983–2001.

Haines, D.A., and Frost, J.S. 1978. Weathering effects on fuel moisture sticks: corrections and recommendations. USDA For. Serv. Res. Pap. NC-154.

Hart, C.A. 1964. Theoretical effect of gross anatomy upon conductivity of wood. For. Prod. J. **14**: 25–32.

Hart, C.A. 1977. Effective surface moisture content of wood during sorption. Wood Sci. **9**(4): 194–201.

Hess, S.L. 1959. Introduction to theoretical meteorology. Holt, Rinehart & Winston, New York.

Jemison, G.M., Lindenmuth, A.W., and Keetch, J.J. 1949. Forest fire-danger measurement in the eastern United States. U.S. Dep. Agric. Agric. Handb. 1.

Katchalsky, A., and Curran, P.F. 1965. Nonequilibrium thermodynamics in biophysics. Harvard University Press, Cambridge, Mass.

Kreith, F. 1967. Principles of heat transfer. 2nd ed. International Textbook Co., Scranton, Pa.

Kreith, F., and Sellers, W.D. 1975. General principles of natural evaporation. *In* Heat and mass transfer in the biosphere. Part 1. Transfer processes in the plant environment. *Edited by* D.A. DeVries and N.H. Afgan. Scripta Book Co., Halstead Press, John Wiley, New York. pp. 207–220.

Moren, T., Salin, J.G., and Soderstrom, O. 1992. Determination of the surface emission factors in wood sorption experiments. *In* Proceedings of the 3rd IUFRO International Wood Drying Conference, 18–21 Aug. 1992, Boku, Vienna, Austria. *Edited by* Manfred Vanek. IUFRO, Vienna. pp. 69–73.

Nelson, R.M., Jr. 1986. Diffusion of bound water in wood. Part 2: A model for isothermal diffusion. Wood Sci. Technol. **20**: 235–251.

Nelson, R.M., Jr. 1991*a*. Heats of transfer and activation energy for bound water diffusion in wood. Wood Sci. Technol. **25**: 193–202.

Nelson, R.M., Jr. 1991*b*. Test of an equation for nonisothermal moisture transport in wood. Wood Sci. Technol. **25**: 321–325.

Parkhurst, W.R., Bahr, R.R., and Johnson, L.W. 1994. A system to remotely sense the moisture levels in 10-hour time-lag fuels. *In* Proceedings of the 12th Conference on Fire and Forest Meteorology, 26–28 Oct. 1993, Jekyll Island, Ga. Society of American Foresters, Bethesda, Md. pp. 787–796.

Patankar, S.V. 1980. Numerical heat transfer and fluid flow. Hemisphere Publishing Corp., New York.

Peralta, P.N. 1995. Modeling wood moisture sorption hysteresis using the independent-domain theory. Wood Fiber Sci. **27**: 250–257.

Peralta, P.N., and Skaar, C. 1993. Experiments on steady-state nonisothermal moisture movement in wood. Wood Fiber Sci. **25**: 124–135.

Plumb, O.A., Spolek, G.A., and Olmstead, B.A. 1985. Heat and mass transfer in wood during drying. Int. J. Heat Mass Transfer, **28**: 1669–1678.

Rosen, H.N. 1982. Predicting wood surface moisture content during water vapor sorption. Wood Sci. **14**(3): 134–137.

Schneider, P.J. 1955. Conduction heat transfer. Addison-Wesley, Reading, Mass.

Shortley, G., and Williams, D. 1955. Elements of physics. 2nd ed. Prentice-Hall, Englewood Cliffs, N.J.

Siau, J.F. 1995. Wood: Influence of moisture on physical properties. Department of Wood Science and Forest Products, Virginia Polytechnic Institute and State University, Blacksburg.

Skaar, C. 1988. Wood-water relations. Springer-Verlag, Berlin.

Spolek, G.A., and Plumb, O.A. 1980. A numerical model of heat and mass transport in wood during drying. *In* Drying, 1980. Hemisphere Publishing Corp., New York. pp. 84–92.

Spolek, G.A., and Plumb, O.A. 1981. Capillary pressure in softwoods. Wood Sci. Technol. **15**: 189–199.

Stamm, A.J. 1959. Bound-water diffusion into wood in the fiber direction. For. Prod. J. **9**(1): 27–32.

Stamm, A.J. 1964. Wood and cellulose science. Ronald Press, New York.

Storey, T.G. 1965. Estimating the fuel moisture content of indicator sticks from selected weather variables. USDA For. Serv. Res. Pap. PSW-26.

Tarkow, H., and Stamm, A.J. 1960*a*. Diffusion through air-filled capillaries of softwoods—part I. Carbon dioxide. For. Prod. J. **10**: 247–250.

Tarkow, H., and Stamm, A.J. 1960*b*. Diffusion through air-filled capillaries of softwoods—part II. Water vapor. For. Prod. J. **10**: 323–324.

Van Wagner, C.E. 1979. A laboratory study of weather effects on the drying rate of jack pine litter. Can. J. For. Res. **9**: 267–275.

Wengert, E.M. 1966. Parameters for predicting maximum surface temperatures of wood in exterior exposures. USDA For. Serv. Res. Pap. FPL-62.

Appendix A

Liquid water transport

Darcy's law, in differential form, states that the flux of a fluid through a porous medium is proportional to the pressure gradient in the fluid. In wood, the law strictly is applicable to saturated flow, but Spolek and Plumb (1980, 1981) assume it describes unsaturated flow also. The same assumption is made here. The flux of liquid water in a 10-h fuel stick (on a whole-wood basis), J ($kg \cdot m^{-2} \cdot h^{-1}$), is given by Darcy's law as

$$[A1] \quad J = -\left(\frac{K}{\nu}\right)\left(\frac{\partial P_l}{\partial r}\right)$$

where K is the stick permeability to liquid flow (eqs. 3 of the text), ν is the liquid water kinematic viscosity (eq. 5 of the text), P_l is the liquid water pressure ($kg \cdot m^{-1} \cdot h^{-2}$), and r is the radial distance from the stick center (m). Capillary pressure, P_c, is related to the gas and liquid phase pressures (P_g and P_l, respectively) within a cell cavity according to

$$[A2] \quad P_c = P_g - P_l = s\left(\frac{1}{r_1} + \frac{1}{r_2}\right)$$

where r_1 and r_2 are radii of curvature of the cavity, m. If movement of the liquid is sufficiently slow, air can diffuse into the cavity, maintaining uniform gas pressure. Thus, P_g is considered constant. Continuity considerations and replacement of $\partial P_l/\partial r$ in eq. A1 by $-\partial P_c/\partial r$ lead to

$$[A3] \quad r\left(\frac{\partial C_l}{\partial t}\right) = r\rho(m_{max} - m_{fsp})\left(\frac{\partial S}{\partial t}\right) = -\frac{\partial[(rK/\nu)(\partial P_c/\partial r)]}{\partial r}$$

where C_l ($kg \cdot m^{-3}$) is the liquid water concentration on a whole-wood basis. Spolek and Plumb (1980) give P_c for two different ranges in S as

$$[A4] \quad P_c = \frac{4s}{w}, \qquad S_c < S < 1$$

$$[A5] \quad P_c = \left(\frac{2s}{w}\right)\left[1 + \left(\frac{S_c}{S}\right)^{0.5}\right], \qquad 0 < S < S_c$$

Equation A4 applies when the meniscus is in the region of the cell cavity where r_1 and r_2 are constant and equal; eq. A5 applies when the meniscus is in the tapered end of the cavity. Differentiation of eqs. A4 and A5 with respect to r and substitution into eq. A3 yields

$$[A6] \quad \frac{\partial S}{\partial t} = 0, \qquad S_c < S < 1$$

$$[A7] \quad r\rho(m_{max} - m_{fsp})\left(\frac{\partial S}{\partial t}\right) = \frac{\partial[(rKs/\nu w S_c)(S_c/S)^{1.5}(\partial S/\partial r)]}{\partial r}, \qquad 0 < S < S_c$$

In the range $0 < S < S_c/4$, in which $\partial P_c/\partial r$ is nonzero, the right side of eq. A7 is zero, because K is zero (from eqs. 3 of the text). Thus, eq. A7 must be partitioned into

$$[A8] \quad r\rho(m_{max} - m_{fsp})\left(\frac{\partial S}{\partial t}\right) = \frac{\partial[(rKs/\nu w S_c)(S_c/S)^{1.5}(\partial S/\partial r)]}{\partial r}, \qquad \frac{S_c}{4} < S < S_c$$

$$[A9] \quad \frac{\partial S}{\partial t} = 0, \qquad 0 < S < \frac{S_c}{4}$$

Equations A6, A8, and A9 make up eqs. 4 of the text.

Flow into surface fiber cavities

Surrounding a 10-h stick immediately after rain is a water film, some of which evaporates into the atmosphere, and some of which enters a thin surface layer of wood because of a difference between pressure in the film and gas pressure in the unsaturated cavities. Pressure in the film is $P_b + s/a$ where P_b is the atmospheric pressure, and s/a is the pressure exerted by film surface tension given by eq. A2 with r_1 equal to stick radius a and r_2, along the stick length, approaching infinity. Pressure in the gas is P_b, so the flow is driven by pressure difference s/a. The long axis of the cell cavity parallels that of the stick. Thus, the transverse flow into a single cavity (or slot) is modeled with Poiseuille flow in short cylindrical capillaries of equal height and

diameter that fill the cavity space (side by side). Cylinder height (the effective capillary length), therefore, is taken as equal to the cavity diameter. The volumetric flow ($m^3 \cdot h^{-1}$) into such a capillary is

$$[A10] \quad V_c = \frac{\pi s r_c^4}{8 a \mu_w d}$$

where r_c is the capillary radius (9.2×10^{-6} m), μ_w the dynamic viscosity of liquid water ($kg \cdot m^{-1} \cdot h^{-1}$), and d the effective capillary length, $2r_c$. This result for a single capillary may be extended to the entire stick surface. The volumetric flow into the stick, V, is given by

$$[A11] \quad V = \left(\frac{2\pi a}{l}\right) V_c = \frac{\pi^2 s r_c^2}{16 \mu_w}$$

where l is the capillary dimension along the stick circumference and equals $2r_c$. Thus the capillary effect may be written, using eq. A11, as

$$[A12] \quad E_c = \frac{\sigma p_w V}{2\pi a L \rho} = \frac{\pi s r_c^2}{16 \nu L \rho a^2}$$

where kinematic viscosity ν comes from eq. 5 of the text, ρ_w is the density of liquid water, L is stick length, and σ is the stick surface-to-volume ratio given by $2/a$. Equation A12 is used as eq. 16 in the text.

Appendix B

Bound water diffusivity

Bound water diffusion in 10-h sticks is strongly dependent upon the wood moisture content fraction, m, and stick temperature, T_s. The bound water diffusivity, D_w, is often expressed on a volume of cell wall basis. Conversion of D_w to a whole-wood diffusivity, D_b, involves the volume fraction of adsorbed water, F_a, and the volume fraction of cell wall substance, F_w. Quantities F_a and F_w are calculated from relationships used by Hart (1964) and Choong (1965). A model for D_w reported by Nelson (1986) is given in units of the present paper by

$$[B1] \quad D_w = 0.071 C \, e^{-E/[R_g(T_s + 273.2)]}$$

where universal gas constant R_g is 8.32 $J \cdot mol^{-1} \cdot K^{-1}$ and C is a correction for diffusion path tortuosity given by

$$[B2] \quad C = (2 - F_a)^{-1}$$

For converting D_w to a whole-wood basis, Siau (1995) uses a multiplier, F, as

$$[B3] \quad F = [F_w(1 - (1 - F_w)^{0.5})]^{-1}$$

Quantity E is the activation energy for bound water diffusion modeled by Nelson (1991*a*) as

$$[B4] \quad E = \frac{[Q_v + Q_w - c_v(T_s + 273.2)]}{1.2}$$

where Q_v is the heat of vaporization of liquid water at temperature T_s ($J \cdot mol^{-1}$), Q_w is the differential heat of sorption ($J \cdot mol^{-1}$), c_v is the constant-pressure specific heat of water vapor at T_s ($J \cdot mol^{-1} \cdot K^{-1}$), and T_s is the stick temperature (°C). Nelson (1991*b*) uses for Q_v and c_v the expressions

$$[B5a] \quad Q_v = 56\,720 - 42.8(T_s + 273.2)$$

$$[B5b] \quad c_v = 30.22 + 0.009\,94\,(T_s + 273.2) + 1.12 \times 10^{-6}\,(T_s + 273.2)^2$$

and Skaar (1988) gives the heat of sorption as

$$[B5c] \quad Q_w = 21\,000 \, e^{-14m}$$

A problem to be considered in modeling D_b is its dependence on the direction of flow with respect to the wood fiber direction. Skaar (1988) states that diffusion across the fibers (averaged for the radial and tangential directions) is about 2.5 times slower than diffusion along the fibers; a factor of 2 was suggested by trials and and is used in the model. Nelson (1986) has shown that expressing eq. B1 on a whole-wood basis leads to a diffusivity that agrees well with experimental bound water diffusivities along the fibers reported by Stamm (1959). Thus, D_b may be approximated as

$$[B6] \quad D_b = \left(\frac{F}{2}\right) D_w = 0.035 C F \, e^{-E/[R_g(T_s + 273.2)]}$$

where the factor "2" corrects for diffusion across the fibers. When the cell wall is saturated, D_b is evaluated by setting moisture fraction m equal to m_{fsp}.

Vapor diffusivity

Vapor diffusion in the cell cavities of 10-h sticks may be analyzed with the equation for diffusion of water vapor in air. The transverse flux of vapor in a cylindrical air space at temperature T_s is

$$[B7] \quad J_a = -\left[\frac{D_a M_w}{R_g(T_s + 273.2)}\right]\left(\frac{dp}{dr}\right)$$

where J_a is the vapor flux in air ($kg \cdot m^{-2} \cdot h^{-1}$), D_a is the diffusivity of water vapor in air ($m^2 \cdot h^{-1}$), M_w is the molecular weight of water (0.018 $kg \cdot mol^{-1}$), R_g is the universal gas constant (1.08×10^8 $kg \cdot m^2 \cdot h^{-2} \cdot mol^{-1} \cdot K^{-1}$), p is the vapor pressure ($kg \cdot m^{-1} \cdot h^{-2}$), and r is the radial coordinate (m). This equation may be converted from a volume of air to a volume of whole wood basis by multiplying it by the stick porosity to give the whole-wood vapor flux, J_v, as

$$[B8] \quad J_v = -\left[D_a M_w (1 - F_w)\frac{P_s}{R_g(T_s + 273.2)}\right]\left(\frac{dH_s}{dm_e}\right)\left(\frac{dm}{dr}\right) = -\rho D_v\left(\frac{dm}{dr}\right)$$

where P_s is the saturation vapor pressure at T_s, ρ is the stick density, H_s is the fractional humidity within the stick, dp is $P_s dH_s$, (dH_s/dm_e) is the reciprocal slope of the sorption isotherm evaluated at T_s, and D_v is the whole-wood vapor diffusivity. Implicit in this equation are the assumptions that the local moisture content fraction m approximates the equilibrium value m_e and that the reciprocal slope normally obtained from measurements of sorption on an entire stick also applies at sites within the stick. These assumptions will tend to be valid because (*i*) the stick is isothermal, (*ii*) the local vapor and bound water phases may be considered to be in thermodynamic equilibrium, and (*iii*) the reciprocal slope of the isotherm is weakly dependent on relative humidity and temperature. Stamm (1964) determines D_a with the equation

$$[B9] \quad D_a = 0.0792\left(\frac{1.31 \times 10^{12}}{P_b}\right)\left(\frac{T_s + 273.2}{273.2}\right)^{1.75}$$

where sea-level atmospheric pressure is 1.31×10^{12} $kg \cdot m^{-1} \cdot h^{-2}$ and P_b is atmospheric pressure at the site in the same units.

Equation B9 describes vapor diffusion in a space as small as a wood cell cavity because the mean free path of the vapor is smaller than the cavity diameter. Tarkow and Stamm (1960*a*), however, found that diffusion of carbon dioxide through the fine capillary structure of Sitka spruce (*Picea sitchensis* (Bong.) Carr.) is smaller by a factor of 40 than diffusion of the free gas because the carbon dioxide must pass through cell wall pit membrane pores that are smaller than the mean free path of its molecules. Thus, a factor to account for hindered (or Knudsen) diffusion of carbon dioxide through Sitka spruce is 0.025. This reduction in diffusion is highly variable among woods and depends on factors such as the fraction of cell wall covered with pits, the fraction of pits that are aspirated, the extent of encrustation of the pit membrane pores, and dimension change with moisture content and temperature. Tarkow and Stamm (1960*b*) also have shown that most of the resistance to transverse vapor diffusion is in the pores. If the diffusion of carbon dioxide and water vapor in air follows Graham's law of diffusion and the correction factors for the two gases are inversely proportional to their diffusivities, then a hindered diffusion correction for water vapor, X, may be estimated as

$$[B10] \quad X = 0.025\left(\frac{M_w}{M_c}\right)^{0.5} = 0.016$$

where M_c is the molecular weight of carbon dioxide (0.044 $kg \cdot mol^{-1}$). When X is introduced, eq. B8 yield a vapor diffusivity given by

$$[B11] \quad D_v = \frac{X D_a M_w (1 - F_w) P_s (dH_s / dm_e)}{\rho R_g (T_s + 273.2)}$$

where D_a and X are obtained from eqs. B9 and B10.

Combined diffusivity

Siau (1995) assumes that the only resistance to vapor diffusion in wood is in the cell cavities; the author, on the other hand, believes that cell cavity resistance controls vapor flow only in the longitudinal direction. For the transverse diffusion occurring in 10-h fuel sticks, it is assumed that bound water moves through crosswalls of the wood fibers in parallel with the hindered diffusion of water vapor through the pit membrane pores. Thus, the combined diffusivity, D, corresponds to conductances in parallel ($D = D_b + D_v$), which is eq. 7 in the text.

Appendix C

Surface heat transfer by vapor exchange

Calculation of the 10-h stick surface temperature T_s can be simplified by expressing the term involving moisture flux G_v in eq. 8 in the text as a temperature difference. The research of Kreith and Sellers (1975) and Hart (1977) makes this possible. The former authors relate G_v to a vapor pressure difference; the latter presents evidence suggesting that the psychrometric equation, an equation usually applied to free-water evaporation, also describes the relationship between vapor pressure and temperature at the surface of wood below the fiber saturation point. Thus, it is assumed that eq. 20 in the text is applicable over the entire range of conditions to which the surface of a 10-h stick can be exposed. This equation may be written in the form

$$[C1] \quad p_s - p_a = P_b A(T_a - T_s)\left(\frac{Q_v}{Q_v + Q_w}\right)$$

where p_a is the ambient vapor pressure. Kreith and Sellers (1975) express G_v as

$$[C2] \quad G_v = \frac{0.622\rho_a D_e(p_s - p_a)}{P_b}$$

where 0.622 is the ratio of molecular weights of water and air, ρ_a is the density of ambient air ($kg \cdot m^{-3}$), and D_e is a transfer coefficient for water vapor ($m \cdot h^{-1}$). Using arguments based on the similarity of heat and mass transfer, Kreith (1967) defines a vapor transfer coefficient, k_g($h \cdot m^{-1}$), such that

$$[C3] \quad k_g = \frac{0.622\rho_a D_e}{P_b} = \frac{0.622 h_c(\mathrm{Pr}/\mathrm{Sc})^{0.667}}{c_a P_b}$$

where c_a is the constant-pressure specific heat of air. It is now postulated that rate eq. C2 is applicable above and below the fiber saturation point, as is the equilibrium relation in eq. C1. Because the rate expression describes a deviation from equilibrium, this assumption is plausible if the deviation is not large (Katchalsky and Curran 1965). Thus, combining eqs. C1–C3 and multiplying by $(Q_v + Q_w)/M_w$ leads to

$$[C4] \quad (Q_v + Q_w)\frac{G_v}{M_w} = \frac{0.622 h_c(\mathrm{Pr}/\mathrm{Sc})^{0.667} Q_v A(T_a - T_s)}{c_a M_w} = h_v(T_a - T_s)$$

where h_v is a heat transfer coefficient associated with vapor exchange given by eq. 10 in the text. Substitution of eq. C4 into eq. 8 in the text leads to eq. 9.

Surface moisture content change involving liquid water

The change in moisture content fraction due to condensation or evaporation of free water at the surface of a 10-h stick during time dt is related to stick density ρ and radius a according to

$$[C5] \quad \mathrm{d}m_s = -2\left(\frac{G_v}{\rho_a a}\right)\mathrm{d}t = -2E_p\ \mathrm{d}t$$

This equation combines with eqs. C2 and C3 and with the equality $p_a = P_d$ (where P_d is the saturation vapor pressure at the dewpoint temperature) to give eq. 15 in the text.